Equilibrium and Kinetic Modeling of Pb(II) Biosorption by a Chemically Modified Orange Peel Containing Cyanex 272[†]

Lili Lü, Lihua Chen, Wenjing Shao, and Fang Luo*

Key Laboratory of Polyoxometalates Science of the Ministry of Education, College of Chemistry, Northeast Normal University, Changchun 130024, China

In this paper, a new kind of biosorbent containing the extractant Cyanex 272 was prepared by the method of solid−liquid grinding and found to be efficient in removing Pb(II) from aqueous solution. Orange peel (OP) biosorbents were characterized by SEM, FTIR, BET, and elemental analysis, which confirmed that carboxylic groups were introduced into the orange peel by chemical modification [citric acid (CO), saponification and citric acid (SCO)] and that Cyanex 272 was successfully immobilized on the orange peel (272OP, 272CO, and 272SCO). In addition, Cyanex 272 played an important role in the adsorption process, i.e., the maximum adsorption capacity (obtained from the Langmuir−Freundlich model) was improved, with the order of the adsorption capacities being 272SCO (1.30 mol·kg^{-1}) > SCO (1.26 mol·kg^{-1}) > 272CO (1.20 mol·kg^{-1}) > 272OP (1.02 mol·kg^{-1}) > CO (0.62 mol·kg^{-1}), and the equilibrium time was shortened from 60 to 40 min for 272SCO. It was obvious that adsorption of Pb(II) strongly depends on pH, with the optimum pH range being 5.0−5.8 for all adsorbents, and the removal rate of Pb(II) by 272SCO could be as high as 100 %. The optimum solid/liquid ratio was 3.7 g·L^{-1} for an initial Pb(II) concentration of 0.002 mol·L^{-1}. The kinetic equilibria could be explained as pseudo-second-order kinetic processes. The optimum desorption agent was found to be 0.1 mol·L^{-1} HCl. The adsorption capacity of 272SCO declined slightly after being recycled six times. After the sixth cycle, the adsorption rate of Pb(II) onto 272SCO was still 89.61 %.

1. Introduction

Heavy-metal pollution in aquatic systems remains a serious environmental and public problem. Heavy-metal ions are often found in the environment as a result of their wide industrial uses. They have been classified as hazardous pollutants because of their potential harmful effects on human health.[1,2] They are harmful to organisms even at low concentrations. In addition, heavy metals are not biodegradable and tend to accumulate in living organisms, causing various diseases and disorders. Therefore, their presence in the environment, particularly in ground waters, should be controlled. Some efficient methods for removing heavy metals from industrial wastewaters have received much more attention over the past decade. Different technologies and processes, such as chemical and electrochemical techniques,[3,4] membrane processes,[5,6] advanced oxidation processes,[7] and biosorption procedures[8−10] are the most widely used for removing metals from industrial effluents. Among all of the proposed treatments, biosorption is a well-known equilibrium separation process that is recognized as an effective, efficient, and economical method for extracting and separating heavy metals. Various biological materials, which have attracted more attention and interest and are available in vast amounts, have emerged as cost-effective and efficient alternatives for treatment of low-strength wastewater as well as certain waste products from industrial and agricultural operations.[11,12] Because of its high toxicity, lead can exert its toxic effects even at low concentrations and seriously endanger the ecological environment and human health.[13] The increasing presence of lead in the environment derives mainly from industrial activities, such as petrol additives, electroplating, paint pigments, alloy preparation, and batteries. With the development of biosorption technology, there are many materials available for removing lead from wastewater, such as *Cephalosporium aphidicola*,[14] citrus pectin,[15] fungal biomass,[16] and olive stone waste.[17] However, exploration and development of new biosorption materials still continues.

Cyanex 272 is a type of acidic organophosphorus extractant that has good chemical stability with respect to heat and hydrolysis and can be completely dissolved in aliphatic and aromatic diluents. Cyanex 272 is widely used in separation and purification of rare-earth elements and other metals.[18−21] In order to reduce the use of toxic, volatile organic solvents, Cyanex 272 has been immobilized onto various supports. Karve and Rajgor[22] reported the use of Amberlite XAD-2 resin impregnated with Cyanex 272 and Cyanex 302 to separate uranium(VI) from rare-earth elements. Sun and co-workers[23] developed a method in which Cyanex923 was fixed on Amberlite XAD-7 with the assistance of an ionic liquid and then used to extract yttrium from rare earths.

In this work, a biomass material with a macroporous structure, high surface area, and good mechanical stability was first chosen as a support to immobilize Cyanex 272; cellulosic orange peel was found to be suitable. Second, in order to improve the performance of the orange peel, it was modified with citric acid to introduce a large number of functional carboxyl groups for binding metal ions. Third, a solid−liquid grinding method was used to immobilize Cyanex 272 on the modified orange peel in order to further enhance the uptake of Pb(II) from aqueous solution. In this work, in view of the cost, the dosage of Cyanex

[†] Part of the "Sir John S. Rowlinson Festschrift".

* Corresponding author. Tel.: +86 431 8889 3336. E-mail: luof746@nenu.edu.cn.

10.1021/je1000846
Published on Web 07/30/2010

272 is very small. Ultimately, a new biosorbent, chemically modified orange peel containing Cyanex 272 was prepared.

2. Experimental Section

2.1. Materials and Reagents. Cyanex 272 (American Cyanamid Company) was used without further purification. The stock solution of Pb(II) was prepared by dissolving a weighed quantity of $PbCl_2$ [Shanghai Reagent Factory (Kunshan factory)] in 25 mL of 0.1 mol·L^{-1} NaCl (Beijing Chemical Works) and 10 mL of hexamethylenetetramine buffer solution (pH 6.4) (Tianjin Huadong Reagents Factory) and then diluting to 250 mL with distilled water. Herein, 0.1 mol·L^{-1} NaCl was used to control the ionic strength and hexamethylenetetramine buffer solution to keep proton balance. The initial pH of each solution was adjusted with 0.1 mol·L^{-1} HCl and/or NaOH (Beijing Chemical Works) and measured with a model pHs-3C acidity meter (Shanghai Precision & Scientific Instrument Co., Ltd.). All of the chemicals used in this study were analytical-grade, and all of the solutions were prepared with distilled water.

2.2. Instrumentation. The morphology of the samples was observed using a field-emission scanning electron microscope (FE-SEM, XL30, Philips). Nitrogen sorption data were obtained with nitrogen gas sorption analyzer (NOVA-1000, Quantachrome Corporation). Elemental analysis of the orange peel was carried out using a GmbH Elementar analyzer by heating the sample from 25 to 1000 °C at a heating rate of 10 °C·min^{-1} and analyzing the gases generated by an electrical conductivity detector. FTIR spectra of the raw, modified orange peel adsorbents and Cyanex 272 were measured with a Fourier transform IR spectrophotometer (Nicolet MagNAIR 560) under ambient conditions. The spectra were recorded from (4000 to 400) cm^{-1} using a KBr disk.

2.3. Preparation of Adsorbents. 2.3.1. Raw Material. Crude orange peel was washed with water to take out silt, sand, and insoluble impurities and then dried for 12 h in a convection oven at a temperature of 60 °C. The dried orange peel was milled, and the smaller particles were obtained using a sieve with a diameter of 0.25 mm. Dried orange peel (30 g) was mixed with 20 % isopropyl alcohol (700 mL) for 24 h at room temperature to remove organic components such as chlorophyll pigments and other low-molecular-weight compounds (e.g., limonene, etc.). The sample was then filtered and washed with distilled water until the filtrate had no color. The residue was dried in an oven at 60 °C for 12 h and used in our experiments as the raw material (designated as OP).

2.3.2. Citric Acid-Modified Material. OP (4 g) and 1.0 mol·L^{-1} citric acid solution (100 mL) were mixed in a beaker and stirred at 60 °C for 2 h and then filtered and dried in a convection oven at 50 °C for 12 h. After that, the product was washed several times with distilled water until the pH was neutral. Finally, the material (designated as CO) was dried in an oven at 60 °C for 12 h.

2.3.3. Citric Acid-Modified Material after Saponification with NaOH. OP (10 g) was added to a beaker together with 0.1 mol·L^{-1} NaOH (200 mL) and stirred for 2 h at room temperature. After filtration, the sample was washed with distilled water until the pH was neutral. The filter residue was dried in an oven at 50 °C for 24 h. Next, the residue was further mixed with 1.0 mol·L^{-1} citric acid solution (70 mL) and stirred for 2 h at 80 °C. The acid/peel slurry was dried overnight at 50 °C in an oven and filtered. Finally, the filter residue was washed with distilled water until the pH was neutral and then dried in an oven for 24 h at 50 °C. This adsorbent is desigated as SCO.

2.3.4. Cyanex 272-Modified Material. Samples (3 g) of OP, CO, and SCO were placed into separate porcelain mortars, and Cyanex 272 (3 mL) was added to each. The solid−liquid mixture was fully ground and then dried for 12 h at 60 °C after aging for 24 h at room temperature. These adsorbents are designated as 272OP, 272CO, and 272SCO, respectively.

2.4. Adsorption Process. Batch adsorption tests were carried out at room temperature and used to investigate the effects of various parameters on Pb(II) adsorption. Each adsorbent (0.025 g) was mixed with Pb(II) aqueous solution (15 mL) in an Erlenmeyer flask, and the mixture was shaken in a rotary shaker for 4 h to reach equilibrium. After filtration through filter paper, 1 mL of filtrate was placed in a conical flask, and 2 drops of 0.1 % xylenol orange, 1 drop of saturated sulfosalicylic acid, and approximately 10 mL of 30 % hexamethylenetetramine solution were added. The concentration of Pb(II) in the filtrate was then determined by titration using a standard EDTA solution. Three separate analyses were performed, and the average was used for this work. The adsorbed amount (q) and the removal efficiency (E) were calculated according to the equations

$$q = \frac{(C_0 - C_e)V}{W} \tag{1}$$

$$E = \frac{C_0 - C_e}{C_0} \times 100 \tag{2}$$

where C_0 and C_e are the initial and equilibrium concentrations (mol·L^{-1}) of Pb(II) in the aqueous phase, respectively, q is the amount of metal ion adsorbed per unit mass of adsorbent (mol·kg^{-1}), W is the mass of adsorbent (kg), and V represents the volume of the aqueous phase (L).

2.5. Desorption Process. Batch desorption tests using different concentrations of HCl were conducted in order to select the optimal concentration of HCl as the eluent in the column tests. After the 0.025 g sample of adsorbent loaded with lead ions was mixed with 15 mL of (0.005, 0.01, 0.05, 0.1, or 0.2) mol·L^{-1} HCl solution in an Erlenmeyer flask, the mixture was shaken in a rotary shaker for 4 h to reach equilibrium. After filtration through filter paper, the concentration of lead in the filtrate was determined by titration using the same method as for the adsorption process.

3. Results and Discussion

3.1. Characterization of Orange Peel. 3.1.1. SEM Image of Orange Peel and Nitrogen Sorption Analysis. Figure 1 shows an SEM image of OP. The surface of OP is irregular and porous, and these macropores and channels are important factors that could lead to high uptake of Pb(II). In addition, this structural feature indicates that OP is competent to be used as a support to fix Cyanex 272. The N_2 adsorption measurements on OP showed that its average pore diameter was 30.50 Å and its specific surface area was 128.70 $m^2 \cdot g^{-1}$.

3.1.2. Elemental Analysis. The elemental analysis results showed that the orange peel was composed of 43.69 % carbon, 5.63 % hydrogen, 47.04 % oxygen, and 3.64 % nitrogen.

3.1.3. FTIR Analysis. To better understand the immobilization of Cyanex 272 on orange peel biosorbents, the FTIR spectra of OP, SCO, 272SCO, and Cyanex 272 were recorded and are compared in Figure 2. The FTIR spectrum of OP (trace a in Figure 2) shows that hydroxyl (−OH) stretch appears at a

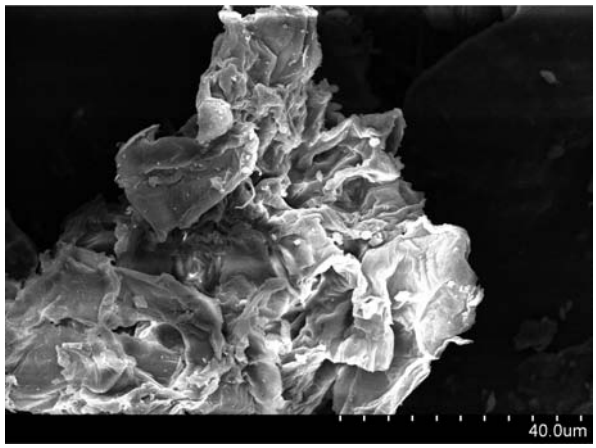

Figure 1. SEM image of OP.

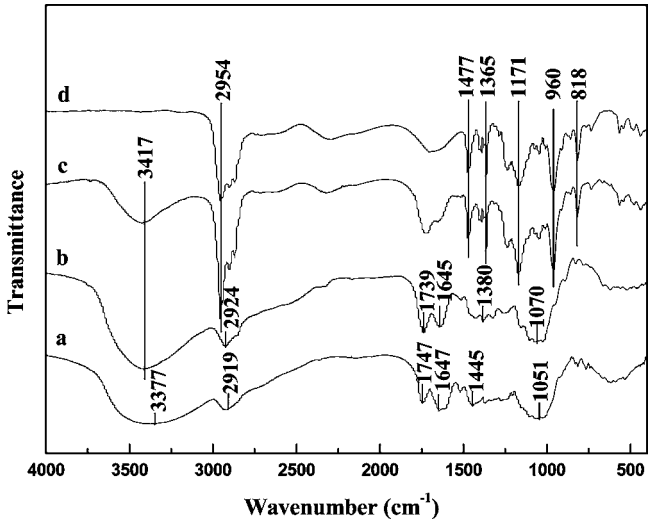

Figure 2. FTIR spectra of (a) OP, (b) SCO, (c) 272SCO, and (d) Cyanex 272.

wavenumber of 3377 cm^{-1}, and the peak at 2919 cm^{-1} is due to the asymmetric and symmetric C−H stretching modes of the aliphatic chains (−CH). The three peaks at (1747 and 1647) cm^{-1} are the carbonyl (C═O) stretching and hydroxyl (−OH) deformation bands of the carboxylic groups. The peak at 1445 cm^{-1} is the symmetric C═O stretch, and the C−O−C vibration appears at 1051 cm^{-1}. For SCO (trace b in Figure 2), it is observed that the hydroxyl (−OH) stretch peak changed to 3417 cm^{-1} as a result of the modification with NaOH; also, the alkyl (−CH) stretch band shifts from (2919 to 2924) cm^{-1} and becomes a broad peak. The hydroxyl (−OH) deformation band of the carboxylic groups shifts a little from (1647 to 1645) cm^{-1}, and the C−O−C vibration shifts to 1070 cm^{-1}. The appearance and disappearance of different peaks indicates that some functional groups (−COOH and −OH) have been successfully introduced into the surface of the orange peel after chemical modification. These functional groups are very effective in capturing Pb(II) ions from aqueous solution. In addition, a comparison of traces c and d in Figure 2 shows that the FTIR spectrum of 272SCO is very similar to that of Cyanex 272 in the fingerprint region, and 272SCO possesses the characteristic peaks of Cyanex 272. For example, the bands at 2954 cm^{-1} can be attributed to −CH stretching of CH_3 contained in the 3-methylamyl group of Cyanex 272, and the two peaks that appear at (1477 and 1365) cm^{-1} are due to the −CH deformation vibration of Cyanex 272. The peak at 1171 cm^{-1} corresponds to the P═O group of Cyanex 272, the C−O−P stretching bands

Table 1. Roles of Different Chemical Reagents in Modifying the Orange Peel

chemical reagent	role
20 % isopropyl alcohol	to discolor the orange peel and remove some polarity and organic small molecule
NaOH	to undergo the cross-linking reaction, increase some active binding sites, and remove further hemicellulose, pigment, etc.
citric acid	to introduce carboxyl (−COOH) groups into cellulose
alkali saponification	to introduce carboxyl groups into the cellulose through alkali saponification
Cyanex 272	to improve its ion-exchange capacity

in 272SCO and Cyanex 272 appear at (960 and 818) cm^{-1}, which remain unaltered. However, the only difference is that at 3417 cm^{-1}, where 272SCO has a band attributed to the hydroxyl (−OH) stretch of CSO but Cyanex 272 does not. This suggests that the Cyanex 272 is fixed to SCO without doubt.

3.2. Adsorption Mechanism. Although biosorption is promising, its mechanism is not well understood. Biosorption probably occurs through a combination of the following mechanisms:[24] chemisorption by ion exchange, complexation, coordination, chelation, physical adsorption, and microprecipitation. However, ion exchange and complexation as the mainstream mechanisms are recognized by colleagues.[25,26] The study of the mechanism of lead biosorption by OP in this work is based on ion exchange. The different modifications were applied to enhance the number of functional groups of cellulose and improve Pb(II) adsorption. Table 1 lists the roles of the different chemical reagents used to modify the orange peel. Functional groups such as −COOH and −OH of cellulose can react with Pb(II) to form complexes by releasing protons.[27] The reactive anhydride combines with cellulosic hydroxyl groups to form an ester linkage and introduce carboxyl groups into the cellulose. The addition of carboxylic functional groups increases adsorbents' abilities to bind with positively charged metal ions.[28,29] Additionally, adsorption capacities are further enhanced because of ion exchange between lead ions and Cyanex 272 fixed on the adsorbents. The pH of the Pb(II) solution decreases after adsorption, and HCl is used as the desorption agent, which indicates that an ion exchange mechanism is involved in the adsorption process.

3.3. Effect of pH on Adsorption. The effect of pH on metal biosorption has been studied previously by many researchers, and the results indicate that the solution pH exerts a great effect on the uptake of metal ions.[30−32] In this work, seven stock solutions of Pb(II) with different initial pH values (1.33, 2.16, 3.23, 4.22, 5.06, 5.49, 6.15) were used to investigate the effect of pH on the adsorption of lead onto different adsorbents. The experimental results are shown in Figure 3.

From Figure 3 we can see that the uptake of lead was small at pH < 2. The reason for this phenomenon is that the competitive adsorption of more hydrogen ions tends to occupy the surface active sites and resist the approach of lead ions because of electrostatic forces, leading to fewer binding sites being available to bind lead ions and thus a very small amount of Pb(II) adsorption. With a pH increase, there are fewer hydrogen ions in solution, which means that there is less competition for binding sites, so more binding sites are available; this leads to an increase in the amount of adsorbed Pb(II) in pH range 3.0−5.0, with the removal percentages reaching a maximum at pH 5.0−6.0. With a further increase in pH, the formation of hydroxyl complexes and precipitation of lead hydroxide result in a decrease in the adsorption efficiency of Pb(II). Figure 3 shows that the removal rate of Pb(II) on 272SCO is 100 % at pH 5.8, and it is clear that the removal

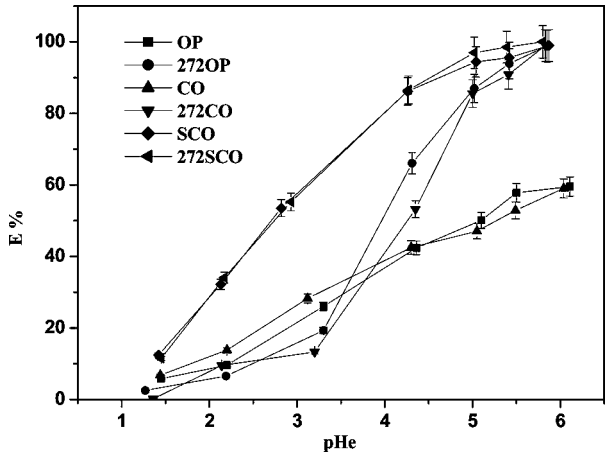

Figure 3. Effect of pH on Pb(II) uptake by different adsorbents. pH_e is the solution pH of the adsorption equilibrium. Initial Pb(II) concentration = 0.001 mol·L^{-1}; solid/liquid (s/l) ratio = 1.6 g·L^{-1}; contact time = 4 h).

Table 2. Parameters for the Pseudo-First-Order and Pseudo-Second-Order Kinetic Models for the Adsorption of Pb(II)

	pseudo-first-order model			pseudo-second-order model		
sorbent type	R^2	q_e/mol·kg^{-1}	k_1/min^{-1}	R^2	q_e/mol·kg^{-1}	k_2/kg·mol^{-1}·min^{-1}
272OP	0.91	0.45	0.18	0.97	0.49	0.59
CO	0.93	0.28	0.11	0.96	0.31	0.49
272CO	0.93	0.45	0.14	0.98	0.49	0.43
SCO	0.96	0.51	0.16	0.97	0.56	0.38
272SCO	0.94	0.54	0.16	0.97	0.59	0.40

rate of Pb(II) on OP is only 59.55 %, which is greatly rises to 98.84 % on 272OP. This suggests that Cyanex 272 plays an important role in the removal of lead ions from aqueous solution.

3.4. Biosorption Kinetics. The contact time was also evaluated as an important factor in the biosorption efficiency; two popularly used kinetic models, pseudo-first-order[33] and pseudo-second-order,[34] were employed to fit the experimental data in this work.

The pseudo-first-order kinetic model is generally expressed through the equation

$$\ln \frac{q_e - q_t}{q_e} = -k_1 t \tag{3}$$

where q_t and q_e are the adsorption amounts of metal ion per unit mass of adsorbent (mol·kg^{-1}) at time t (min) and equilibrium, respectively, and k_1 is the pseudo-first-order rate constant (min^{-1}).

The pseudo-second-order kinetic model is expressed as follows:

$$\frac{t}{q_t} = \frac{1}{k_2 q_e^{\,2}} + \frac{t}{q_e} \tag{4}$$

where k_2 is the pseudo-second-order rate constant (kg·mol^{-1}·min^{-1}).

The kinetic-model parameters obtained from fitting the data are presented in Table 2. The pseudo-second-order kinetic model provides much better R^2 values (0.97, 0.96, 0.98, 0.97, and 0.97) than the pseudo-first-order kinetic model (0.91, 0.93, 0.93, 0.96, and 0.94); this indicates that the pseudo-second order equation was the best fit for the experimental kinetic data, suggesting that chemical sorption is the rate-limiting step of the adsorption mechanism and that there is no involvement of a mass transfer in solution.[35,36]

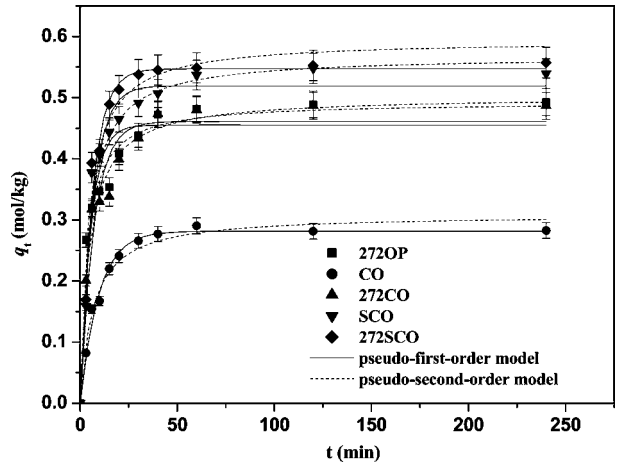

Figure 4. Effect of contact time on Pb(II) uptake by different adsorbents (initial pH = 5.3; initial Pb(II) concentration = 0.001 mol·L^{-1}; s/l ratio = 1.6 g·L^{-1}).

Figure 4 shows the effect of contact time on the adsorption of Pb(II) onto the orange peel adsorbents. It is obvious that more than 60 min was needed to attain equilibrium with OP and SCO, but the equilibrium time was shortened to 40 min for 272OP, 272CO, and 272SCO, which may be attributed to their additional ion exchange capacities. The time-course adsorption data demonstrate that adsorption of Pb(II) occurred rapidly within the first 15 min. The adsorption process of Pb(II) onto orange peel adsorbents seemed to have a second adsorption phase, and it is suspected that the uptake of heavy metals by the orange peel was probably due to not only cell-surface binding but also intracellular accumulation.[37] This possibility was explored by plotting the uptake (q_t) versus $t^{1/2}$, since according to the Weber−Morris model,[38] $q_t = K_{id} \cdot t^{1/2}$, where K_{id} is the intraparticle diffusion coefficient. According to this model, the plot of q_t versus $t^{1/2}$ should be linear if intraparticle diffusion is involved in the adsorption process, and if the plot passes through the origin, then intraparticle diffusion is the rate-controlling step. When the plot does not pass through the origin, this is indicative of some degree of boundary-layer control and further shows that the intraparticle diffusion is not the only rate-limiting step (i.e., there may also be other kinetic models that control the rate of adsorption, all of which may be operating simultaneously).[39] The plots of q_t versus $t^{1/2}$ are presented in Figure 5. It can be seen that these plots do not pass through the origin, which indicates that intraparticle diffusion is not the only rate-controlling step.

3.5. Adsorption Isotherms. The capacity of an adsorbent can be described by sorption isotherms, which can help us explore the adsorption mechanism more deeply. Sorption isotherm equations can explain the adsorption process under equilibrium conditions and provide an easier solution to the complex problem. The Langmuir, Freundlich, and Langmuir−Freundlich models were employed to fit the experimental data in our work. The curves showing the relationship between q_e and the equilibrium concentration of Pb(II) that were obtained from fits to the three isotherms are shown in Figure 6, and the various parameters of isotherm equations are listed in Table 3.

The Langmuir isotherm describes monolayer coverage of adsorbate over specific homogeneous sites, which are assumed to be identical, energetically equivalent, and sufficiently distant

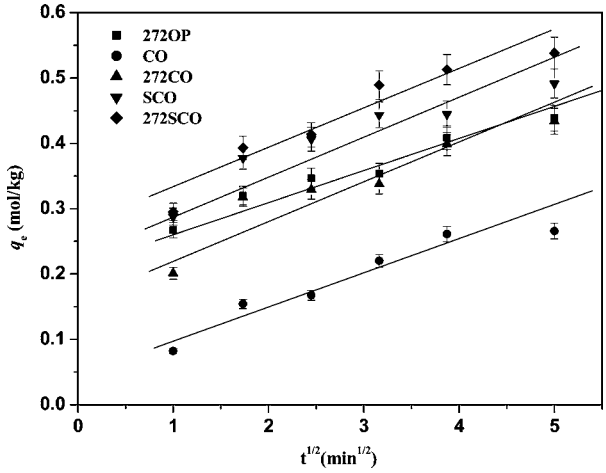

Figure 5. Intraparticle diffusion plots for Pb(II) adsorption by different adsorbents (initial pH = 5.3; initial Pb(II) concentration = 0.001 mol·L^{-1}; s/l ratio = 1.6 g·L^{-1}).

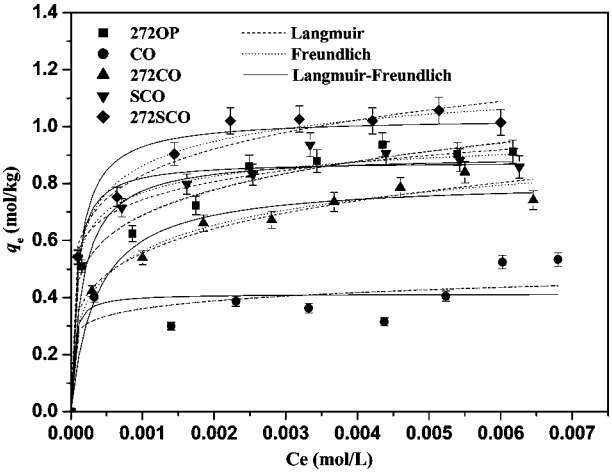

Figure 6. Isotherms for adsorption of Pb(II) by different adsorbents (initial pH = 4.8; s/l ratio = 1.6 g·L^{-1}; contact time = 4 h).

Table 3. Comparison of Three Isotherm Models for Pb(II) Adsorption on Adsorbents

model	parameter	272OP	CO	272CO	SCO	272SCO
Langmuir	R^2	0.94	0.74	0.96	0.97	0.97
	b/L·mol^{-1}	6156	26042	2830	13958	9268
	q_m/mol·kg^{-1}	0.89	0.41	0.81	0.87	1.02
Freundlich	R^2	0.98	0.78	0.98	0.98	0.98
	K_f/L·kg^{-1}	2.32	0.74	2.28	1.68	2.36
	n	5.67	9.48	4.88	8.45	6.59
L−F	R^2	0.98	0.96	0.98	0.98	0.99
	b/L·mol^{-1}	8.98	4.88	12.9	39.9	42.5
	n	2.86	2.62	2.46	2.48	2.24
	q_m/mol·kg^{-1}	1.02	0.62	1.20	1.26	1.30

from each other that there are no interactions between molecules adsorbed on neighboring sites:[40]

$$q_e = \frac{q_m b C_e}{1 + bC_e} \tag{5}$$

where q_e and q_m (mol·kg^{-1}) are the equilibrium and maximum adsorption amounts of metal ion per unit mass of adsorbent, respectively, b represents the equilibrium constant of the adsorption reaction, and C_e (mol·L^{-1}) is the concentration of adsorbate at equilibrium. The R^2 values of the Langmuir isotherms were 0.94, 0.74, 0.96, 0.97, and 0.97 for Pb(II) adsorption on 272OP, CO, 272CO, SCO, and 272SCO, respectively, as shown in Table 3. These results indicate that the biosorption of Pb(II) onto orange peel adsorbents fitted the Langmuir model well. In other words, this adsorption process took place at the functional groups/binding sites on the surface of the adsorbents, which is regarded as monolayer biosorption.

Table 4. Literature Results for Pb(II) Ion Biosorption by Various Sorbents

sorbent material	sorption capacity/mg·g^{-1}	reference
saw dust (*Pinus sylvestris*)	22.22	45
tea waste	65.00	46
modified peanut husk	29.14	47
Symphoricarpus albus	62.16	48
Streptomyces noursei	36.50	49
Rhizopus arrhizus	55.60	50
Cephalosporium aphidicola	36.91	14
grape stalk waste	49.93	51
Penicillium simplicissimum	76.90	52
272SCO	269.4	this study

The Freundlich isotherm[41] is an empirical equation based on the assumption that the adsorption process takes place on heterogeneous surfaces and the adsorption capacity is related to the concentration of lead at equilibrium:

$$q_e = K_f C_e^{1/n} \tag{6}$$

where K_f and n are the Freundlich constants. K_f is a rough indicator of the adsorption capacity (L·kg^{-1}), and $1/n$ is an empirical parameter relating to the adsorption intensity. The values of n were found to be 5.67, 9.48, 4.88, 8.45, and 6.59 for Pb(II) adsorption onto 272OP, CO, 272CO, SCO, and 272SCO, respectively. They were between 1 and 10 for all of the adsorbents, indicating that the adsorption performance of Pb(II) on all of the orange peel adsorbents was favorable under the studied conditions.[39,42]

The Langmuir−Freundlich (L−F) isotherm is given by the expression[43]

$$q_e = q_m \frac{bC_e^{1/n}}{1 + bC_e^{1/n}} \tag{7}$$

in which n is the L−F constant. On the basis of a comparison study of a number of isotherm equations applied to the sorption of Cd(II) and Pb(II) onto brown seaweed, Basha and Jha[44] concluded that the L−F isotherm provided the best fit of the experimental data ($R^2 = 0.9747$). In our study, the values of R^2 were 0.98, 0.96, 0.98, 0.98, and 0.99 for Pb(II) adsorption on 272OP, CO, 272CO, SCO, and 272SCO, respectively, suggesting that the L−F isotherm fit the experimental data the best. The order of the maximum capacities q_m of Pb(II) onto different adsorbents was 272SCO (1.30 mol·kg^{-1}) > SCO (1.26 mol·kg^{-1}) > 272CO (1.20 mol·kg^{-1}) > 272OP (1.02 mol·kg^{-1}) > CO (0.62 mol·kg^{-1}). A comparison of our adsorbents with others is provided in Table 4, and the biosorption capacity of 272SCO obtained for lead(II) ions in our study was found to be higher than that of sorbents in the literature.

3.6. Effects of Solid/Liquid Ratio on Pb(II) Adsorption. The influence of solid/liquid (s/l) ratio on the adsorption of Pb(II) was investigated and is shown in Figure 7. In a system of batch experiments, various s/l ratios were tested to evaluate the optimum adsorbent mass per unit solution volume at an initial Pb(II) concentration of 0.002 mol·L^{-1}. It is to be noted from

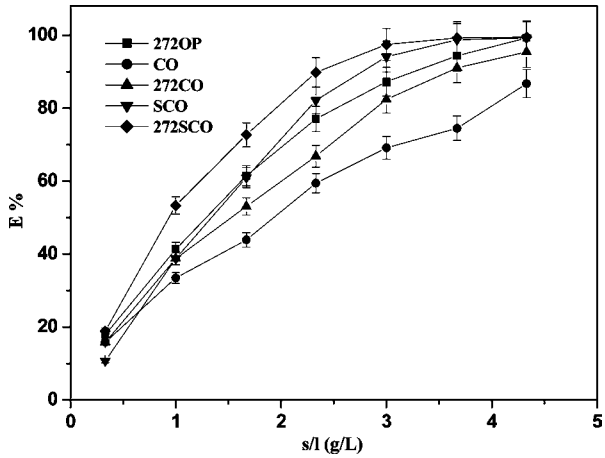

Figure 7. Effect of s/l ratio on Pb(II) adsorption by chemically modified adsorbents (initial Pb(II) concentration = 0.002 mol·L^{-1}; initial pH = 4.8; contact time = 4 h).

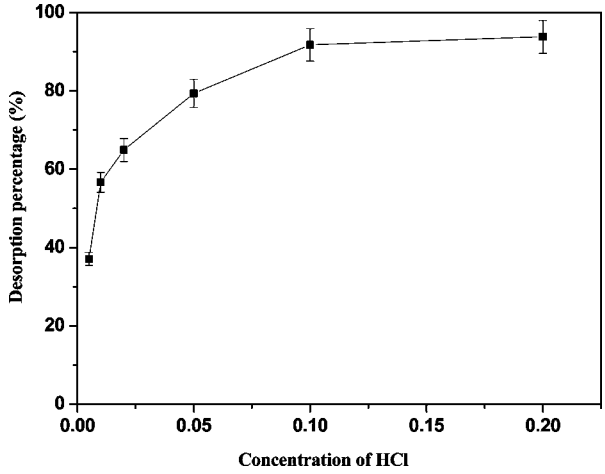

Figure 8. Effect of concentration of HCl on desorption percentage by 272SCO (s/l ratio = 1.60 g·L^{-1}; contact time = 4 h).

the results that the removal percentages of Pb(II) increased with increasing s/l ratio and then changed little after the s/l ratio reached a particular value. The maximum adsorption capacity was almost 100 % when the s/l ratio was 3.7 g·L^{-1}. In terms of removal percentage and cost effect, the optimum s/l ratio was 3.7 g·L^{-1}.

3.7. Regeneration and Recycled Use of Adsorbents. The performance of an adsorbent after regeneration is an important characteristic to explore. An adsorbent with fine regeneration capacity can reduce pretreatment costs and has good practical application. In this study, desorption experiments were conducted under different concentrations of HCl. From Figure 8, the percentages of desorption increased with increasing HCl concentration from (0.005 to 0.1) mol·L^{-1} and then changed little and was almost 100 % for HCl concentrations from (0.1 to 0.2) mol·L^{-1}. Therefore, 0.1 mol·L^{-1} HCl is regarded as the optimum desorption concentration. The adsorption capacity of the recycled biosorbent was investigated over six cycles, and the results are shown in Table 5. From Table 5, it is clear that the adsorption capacity of 272SCO has only a small decline after six cycles. After the sixth cycle, the adsorption rate of Pb(II) onto 272SCO was still 89.61 %, which implies that 272SCO has a higher recycling value and wide prospects for practical application.

Table 5. Adsorption−Desorption Recycling of 272SCO

	cycle number					
	1	2	3	4	5	6
adsorption rate (%)[a]	98.81	98.48	98.28	96.35	93.75	89.61
desorption rate (%)[b]	94.50	95.76	92.74	94.85	92.89	94.77

[a] Initial pH = 5.3; initial Pb(II) concentration = 0.001 mol·L^{-1}; s/l ratio = 1.6 g·L^{-1}. [b] Using 0.1 mol·L^{-1} HCl as the desorption agent.

4. Conclusion

In conclusion, a newly developed biosorbent containing the extractant Cyanex 272 has been prepared via a solid−liquid grinding method. Orange peel biosorbents were characterized by SEM, FTIR, BET, and elemental analysis, which confirmed that carboxylic groups were introduced into orange peel by chemical modification and that Cyanex 272 was successfully immobilized on the orange peel. It is clear that adsorption of Pb(II) strongly depends on pH, and the optimum pH is in the range 5.0−5.8 for all of the adsorbents; the removal rate of Pb(II) by 272SCO could be up to 100 %. Kinetic equilibria could be explained as pseudo-second-order kinetic processes. The equilibrium time was shortened from 60 min (without Cyanex 272) to 40 min (with Cyanex 272). The adsorption process was best described using the Langmuir−Freundlich model, and the order of the maximum adsorption capacities was 272SCO (1.30 mol·kg^{-1}) > SCO (1.26 mol·kg^{-1}) > 272CO (1.20 mol·kg^{-1}) > 272OP (1.02 mol·kg^{-1}) > CO (0.62 mol·kg^{-1}); the optimum s/l ratio was 3.7 g·L^{-1} for an initial Pb(II) concentration of 0.002 mol·L^{-1}. The optimum desorption agent was found to be 0.1 mol·L^{-1} HCl, and the desorption rate was 95.58 %. Repeated-use experiments indicated that the adsorption capacity of 272SCO had only a small decline after six cycles, where the adsorption rate of Pb(II) onto 272SCO was still 89.61 %. This new kind of adsorbent could be regarded as a low cost, efficient material for removal of Pb(II) with a higher recycling value. In addition, we will devote ourselves to looking for some new ways to form chemical bond linkages between extractant and biomaterial in our future work.

Literature Cited

(1) Van der Oost, R.; Beyer, J.; Vermeulen, N. P. E. Fish bioaccumulation and biomarkers in environmental risk assessment: A review. *Environ. Toxicol. Pharmacol.* **2003**, *13*, 57–149.
(2) Bagheri, H.; Saraji, M. New polymeric sorbent for the solid-phase extraction of chlorophenols from water samples followed by gas chromatography−electron-capture detection. *J. Chromatogr., A* **2001**, *910*, 87–93.
(3) Chen, X.; Chen, G.; Yue, P. L. Novel electrode system for electroflotation of wastewater. *Environ. Sci. Technol.* **2002**, *36*, 778–783.
(4) Hu, C. Y.; Lo, S. L.; Kuan, W. H. Effects of co-existing anions on fluoride removal in electrocoagulation (EC) process using aluminum electrodes. *Water Res.* **2003**, *37*, 4513–4523.
(5) Cassano, A.; Molinari, R.; Romano, M.; Drioli, E. Treatment of aqueous effluents of the leather industry by membrane processes: A review. *J. Membr. Sci.* **2001**, *181*, 111–126.
(6) Van Der Bruggen, B.; Vandecasteele, C. Removal of pollutants from surface water and groundwater by nanofiltration: Overview of possible applications in the drinking water industry. *Environ. Pollut.* **2003**, *122*, 435–445.
(7) Torrades, F.; Peŕez, M.; Mansilla, H. D.; Peral, J. Experimental design of Fenton and photo-Fenton reactions for the treatment of cellulose bleaching effluents. *Chemosphere* **2003**, *53*, 1211–1220.
(8) Li, Q. B.; Wu, S. T.; Liu, G.; Liao, X. K.; Deng, X.; Sun, D. H.; Hu, Y. L.; Huang, Y. L. Simultaneous biosorption of cadmium(II) and lead(II) ions by pretreated biomass of *Phanerochaete chrysosporium*. *Sep. Purif. Technol.* **2004**, *34*, 135–142.
(9) Li, X.; Tang, Y.; Cao, X.; Lu, D.; Luo, F.; Shao, W. Preparation and evaluation of orange peel cellulose adsorbents for effective removal of cadmium, zinc, cobalt and nickel. *Colloids Surf., A* **2008**, *317*, 512–521.

(10) Yetis, U.; Dolek, A.; Dilek, F. B.; Ozcengiz, G. The removal of Pb(II) by *Phanerochaete chrysosporium*. *Water Res.* **2000**, *34*, 4090–4100.
(11) Srivastava, V. C.; Mall, I. D.; Mishra, I. M. Equilibrium Modeling of Ternary Adsorption of Metal Ions onto Rice Husk Ash. *J. Chem. Eng. Data* **2009**, *54*, 705–711.
(12) Wu, Y.; Zhang, L.; Gao, C.; Ma, J.; Ma, X.; Han, R. Adsorption of Copper Ions and Methylene Blue in a Single and Binary System on Wheat Straw. *J. Chem. Eng. Data* **2009**, *54*, 3229–3234.
(13) Krishnani, K. K.; Ayyappan, S. Heavy metals remediation of water using plants and lignocellulosic agrowastes. *Rev. Environ. Contam. Toxicol.* **2006**, *188*, 59–84.
(14) Tunali, S.; Akar, T.; Ozcan, A. S.; Kiran, I.; Ozcan, A. Equilibrium and kinetics of biosorption of lead(II) from aqueous solutions by *Cephalosporium aphidicola*. *Sep. Purif. Technol.* **2006**, *47*, 105–112.
(15) Balarial, A.; Schiewer, S. Assessment of biosorption mechanism for Pb binding by citrus pectin. *Sep. Purif. Technol.* **2008**, *63*, 577–581.
(16) Svecova, L.; Spanelova, M.; Kubal, M.; Guibal, E. Cadmium, lead and mercury biosorption on waste fungal biomass issued from fermentation industry. I. Equilibrium studies. *Sep. Purif. Technol.* **2006**, *52*, 142–153.
(17) Fiol, N.; Villaescusa, I.; Martiñez, M.; Miralles, N.; Poch, J.; Serarols, J. Sorption of Pb(II), Ni(II), Cu(II) and Cd(II) from aqueous solution by olive stone waste. *Sep. Purif. Technol.* **2006**, *50*, 132–140.
(18) Taghizadeh, M.; Ghasemzadeh, R.; Ashrafizadeh, S. N.; Ghannadi, M. Stoichiometric relation for extraction of zirconium and hafnium from acidic nitrate solutions with Cyanex 272. *Hydrometallurgy* **2009**, *96*, 77–80.
(19) Sun, X.; Wang, J.; Li, D.; Li, H. Synergistic extraction of rare earths by mixture of bis(2,4,4-trimethylpentyl)phosphinic acid and *sec*-nonylphenoxyacetic acid. *Sep. Purif. Technol.* **2006**, *50*, 30–34.
(20) Xiong, Y.; Wang, X.; Li, D. Synergistic extraction and separation of heavy lanthanide by mixtures of bis(2,4,4-trimethylpentyl)phosphinic acid and 2-ethylhexylphosphinic acid mono-2-ethylhexyl ester. *Sep. Purif. Technol.* **2005**, *40*, 2325–2336.
(21) Jia, Q.; Li, D.; Niu, C. Synergistic extraction of zinc(II) by mixtures of primary amine N1923 and Cyanex 272. *Solvent Extr. Ion Exch.* **2002**, *20*, 751–764.
(22) Karve, M.; Rajgor, R. V. Amberlite XAD-2 impregnated organophosphinic acid extractant for separation of uranium(VI) from rare earth elements. *Desalination* **2008**, *232*, 191–197.
(23) Sun, X. Q.; Peng, B.; Ji, Y.; Chen, J.; Li, D. Q. The solid−liquid extraction of yttrium from rare earths by solvent (ionic liquid) impregnated resin coupled with complexing method. *Sep. Purif. Technol.* **2008**, *63*, 61–68.
(24) Volesky, B. Detoxification of metal-bearing effluents: biosorption for the next century. *Hydrometallurgy* **2001**, *59*, 203–216.
(25) Lesmana, S. O.; Febriana, N.; Soetaredjo, F. E.; Sunarso, J.; Ismadji, S. Studies on potential applications of biomass for the separation of heavy metals from water and wastewater. *Biochem. Eng. J.* **2009**, *44*, 19–41.
(26) Sud, D.; Mahajan, G.; Kaur, M. P. Agricultural waste material as potential adsorbent for sequestering heavy metal ions from aqueous solutions: A review. *Bioresour. Technol.* **2008**, *99*, 6017–6027.
(27) Lu, D. D.; Cao, Q. L.; Cao, X. J.; Luo, F. Removal of Pb(II) using the modified lawny grass: Mechanism, kinetics, equilibrium and thermodynamic studies. *J. Hazard. Mater.* **2009**, *166*, 239–247.
(28) Wing, R. E.; Sessa, D. J.; Willet, J. L. Thermochemical conversion of biomass to value-added ion exchange materials. In *Making a Business from Biomass in Energy, Environment, Chemicals, Fibers and Materials*; Overend, R. P., Chornet, E., Eds.; Elsevier: Oxford, U.K., 1997; pp 1015−1022.
(29) Marshall, W. E.; Wartelle, L. H.; Boler, D. E.; Johns, M. M.; Toles, C. A. Enhanced metal adsorption by soybean hulls modified with citric acid. *Bioresour. Technol.* **1999**, *69*, 263–268.
(30) Utomo, H. D.; Hunter, K. A. Adsorption of divalent copper, zinc, cadmuim and lead ions from aqueous solution by waste tea and coffee adsorbents. *Environ. Technol.* **2006**, *27*, 25–32.
(31) Kao, W. C.; Wu, J. Y.; Chang, C. C.; Chang, J. S. Cadmium biosorption by polyvinyl alcohol immobilized recombinant *Escherichia coli*. *J. Hazard. Mater.* **2009**, *169*, 651–658.
(32) Vimala, R.; Das, N. Biosorption of cadmium(II) and lead(II) from aqueous solutions using mushrooms: A comparative study. *J. Hazard. Mater.* **2009**, *168*, 376–382.
(33) Lagergren, S. About the theory of so-called adsorption of soluble substances. *K. Sven. Vetenskapsakad. Handl.* **1898**, *24*, 1–39.
(34) Ho, Y. S.; McKay, G. Sorption of dye from aqueous solution by peat. *Chem. Eng. J.* **1998**, *70*, 115–124.
(35) Yurdakoc, M.; Scki, Y.; Yuedakoc, S. K. Kinetic and thermodynamic studies of boron removal by Siral 5, Siral 40, and Srial 80. *J. Colloid Interface Sci.* **2005**, *286*, 440–446.
(36) Wu, F. C.; Tseng, R. L.; Juang, R. S. Kinetic modeling of liquid-phase adsorption of reactive dyes and metal ions on chitosan. *Water Res.* **2001**, *35*, 613–618.
(37) Bajpai, S. K.; Rohit, V. K. Cation exchanger sawdust (CESD) as an effective sorbent for removal of Cu(II) from aqueous solution. *EJEAFChe, Electron. J. Environ., Agric. Food Chem.* **2007**, *6*, 2053–2065.
(38) Weber, W. J.; Morris, J. C. Kinetics of adsorption on carbon solution. *J. Sanit. Eng. Div., Am. Soc. Civ. Eng.* **1963**, *89*, 31–59.
(39) Hameed, B. H. Equilibrium and kinetic studies of methyl violet sorption by agricultural waste. *J. Hazard. Mater.* **2008**, *154*, 204–212.
(40) Langmuir, I. The constitution and fundamental properties of solids and liquids. *J. Am. Chem. Soc.* **1916**, *38*, 2221–2295.
(41) Freundlich, H. M. F. Uber die adsorption in lasugen. *Z. Phys. Chem.* **1906**, *57*, 385–470.
(42) Treybal, R. E. *Mass Transfer Operations*, 2nd ed.; McGraw Hill: New York, 1968.
(43) Sips, R. Structure of a catalyst surface. *J. Chem. Phys.* **1948**, *16*, 490–495.
(44) Basha, S.; Jha, B. Estimation of Isotherm Parameters for Biosorption of Cd(II) and Pd(II) onto Brown Seaweed, *Lobophora variegate*. *J. Chem. Eng. Data* **2008**, *53*, 449–455.
(45) Taty-Costodes, V. C.; Fauduet, H.; Porte, C.; Delacroix, A. Removal of Cd(II) and Pb(II) ions from aqueous solutions, by adsorption onto saw dust of *Pinus sylvestris*. *J. Hazard. Mater.* **2003**, *105*, 121–142.
(46) Amarasinghe, B. M. W. P. K.; Williams, R. A. Tea waste as a low cost adsorbent for the removal of Cu and Pb from wastewater. *Chem. Eng. J.* **2007**, *132*, 299–309.
(47) Li, Q.; Zhai, J.; Zhang, W.; Wang, M.; Zhou, J. Kinetic studies of adsorption of Pb(II), Cr(III) and Cu(II) from aqueous solution by sawdust and modified peanut husk. *J. Hazard. Mater.* **2007**, *141*, 163–167.
(48) Akar, S. T.; Gorgulu, A.; Anilan, B.; Kaynak, Z.; Akar, T. Investigation of the biosorption characteristics of lead(II) ions onto *Symphoricarpus albus*: Batch and dynamic flow studies. *J. Hazard. Mater.* **2009**, *165*, 126–133.
(49) Mattuschka, B.; Straube, G. Biosorption of metals by a waste biomass. *J. Chem. Technol. Biotechnol.* **1993**, *58*, 57–63.
(50) Fourest, E.; Roux, J. C. Heavy metal biosorption by fungal mycelial by-products: Mechanisms and influence of pH. *Appl. Microbiol. Biotechnol.* **1992**, *37*, 399–403.
(51) Maria, M.; Nuria, M.; Soraya, H.; Nuria, F.; Isabel, V.; Jordi, P. Removal of lead(II) and cadmium(II) from aqueous solutions using grape stalk waste. *J. Hazard. Mater.* **2006**, *133*, 203–211.
(52) Fan, T.; Liu, Y.; Feng, B.; Zeng, G.; Yang, C.; Zhou, M.; Zhou, H.; Tan, Z.; Wang, X. Biosorption of cadmium(II), zinc(II) and lead(II) by *Penicillium simplicissimum*: Isotherms, kinetics and thermodynamics. *J. Hazard. Mater.* **2008**, *160*, 655–661.

Received for review January 26, 2010. Accepted July 17, 2010. We thank the Training Fund of NENU's Scientific Innovation Project (NENU-STC08008) and the Analysis and Testing Foundation of Northeast Normal University.

JE1000846